

Stochastic response of large structures to multiple excitations

Hong Hao¹

ABSTRACT

A multiply-supported rigid plate to spatially correlated ground excitations are analysed. Quasi-static, dynamic and total structural responses are calculated. Different ground motion assumptions are: general case, neglecting phase shifts, neglecting coherency losses and neglecting propagation effects (single input). The results are compared. Some general conclusions on structural responses to correlated multiple ground excitations are drawn.

INTRODUCTION

Large structures, such as bridges, pipelines, will be affected by ground motion propagation. The properties of ground motion propagation have been studied based on the actual recorded data at a high density earthquake accelerometer array, SMART-1. Among those studies, Harichandran and Vanmarcke (1984) proposed a one-dimensional coherency model. Hao, et al. (1989) proposed a two-dimensional coherency model. Using the coherency model (Harichandran and Vanmarcke 1984), Harichandran and Wang (1988; 1990) calculated the responses of a single-span beam and a double-span beam to spatially correlated multiple excitations. Zerva (1990) calculated the responses of a continuous beam using an assumed coherency model. Using the coherency model (Hao, et al. 1989), Hao (1991) analysed a two-dimensional multiply-supported rigid plate to multiple excitations by assuming the ground motion propagating along x direction, Fig. 1. Hao (1989) also simulated spatially correlated ground motion time histories based on the both one- and two-dimensional coherency models mentioned above, and calculated the structural response time histories by using those simulated ground motions as multiple inputs.

In this paper, a multiply-supported rigid plate to multiple excitations is analysed. The two-dimensional coherency model (Hao, et al. 1989) is used. The ground motion propagation direction is arbitrary. Quasi-static, dynamic and total structural responses are calculated. Three cases of ground motion inputs are: Case 1, multiple inputs with both phase shifts and coherency losses, Case 2, multiple inputs with coherency losses only, and Case 3, multiple inputs with phase shifts only. The results from these three cases are normalized by the corresponding results from single input. The normalized results are compared. Some general conclusions on the effects of multiple inputs on structural responses are obtained.

¹ Lecturer, School of Civil and Structural Engrg., Nanyang Technological Institute, Nanyang Ave., Singapore 2263

GROUND MOTION MODEL

Assume earthquake ground motions are stationary and ergodic, the power spectral density function of ground accelerations can be expressed as (Hao 1991)

$$S_{kl}(i\omega) = |H_1(i\omega)|^2 S_0(\omega) |\gamma_{kl}(\omega, d_{kl}^l, d_{kl}^t)| \exp(i\omega d_{kl}^l/v) \quad (1)$$

where ω is circular frequency, v is apparent velocity, $|H_1(i\omega)|^2$ is a highpass filter, which has the form (Ruiz and Penzien 1969)

$$|H_1(i\omega)|^2 = \frac{\omega^4}{(\omega_1^2 - \omega^2)^2 + 4\xi_1^2 \omega_1^2 \omega^2} \quad (2)$$

where the optimal values are $\omega_1 = 1.636$ rad/s and $\xi_1 = 0.619$.

$S_0(\omega)$ is a Kanai-Tajimi power spectral density function given as (Tajimi 1960)

$$S_0(\omega) = \frac{1 + 4\xi_g^2 \frac{\omega^2}{\omega_g^2}}{(1 - \frac{\omega^2}{\omega_g^2})^2 + 4\xi_g^2 \frac{\omega^2}{\omega_g^2}} S \quad (3)$$

where ξ_g is damping ratio, ω_g is central frequency, and S is a scale factor.

The coherency loss function has the form (Hao, et al. 1989)

$$|\gamma_{kl}(\omega, d_{kl}^l, d_{kl}^t)| = \exp(-\beta_1 |d_{kl}^l| - \beta_2 |d_{kl}^t|) \exp \left\{ - \left[\alpha_1(\omega) \sqrt{|d_{kl}^l|} + \alpha_2(\omega) \sqrt{|d_{kl}^t|} \right] \left(\frac{\omega}{2\pi} \right)^2 \right\} \quad (4)$$

where d_{kl}^l and d_{kl}^t are projected distances between the two stations to ground motion propagation direction and its transverse direction, respectively; β_1 and β_2 are constants; $\alpha_1(\omega)$ and $\alpha_2(\omega)$ are given as (Hao 1989)

$$\begin{aligned} \alpha_1(\omega) &= \frac{2\pi a}{\omega} + \frac{b\omega}{2\pi} + c \\ \alpha_2(\omega) &= \frac{2\pi d}{\omega} + \frac{e\omega}{2\pi} + g \end{aligned} \quad 0.314 \leq \omega \leq 62.83 \quad (5)$$

where a , b , c , d , e and g are constants.

By processing the recorded horizontal motions of Event 40 at SMART-1 array, the above constants obtained are (Hao 1989): $\beta_1 = 9.323 \times 10^{-5}$, $\beta_2 = 1.421 \times 10^{-4}$, $a = 1.037 \times 10^{-2}$, $b = 9.33 \times 10^{-5}$, $c = -1.821 \times 10^{-3}$, $d = 8.09 \times 10^{-3}$, $e = 4.083 \times 10^{-5}$ and $g = -1.007 \times 10^{-3}$.

DYNAMIC RESPONSE EQUATIONS

The equations of motion of the rigid plate shown in Fig. 1 can be derived (Hao 1991). The total structural response equations are

$$M_{ss} \ddot{U}^t + C_{ss} \dot{U}^t + K_{ss} U^t = -K_{sb} V_g \quad (6)$$

The dynamic response equations are

$$M_{ss}\ddot{U} + C_{ss}\dot{U} + K_{ss}U = M_{ss}K_{ss}^{-1}K_{sb}\ddot{V}_g \quad (7)$$

and the quasi-static response equations are

$$U^{qs} = -K_{ss}^{-1}K_{sb}V_g \quad (8)$$

where C_{ss} is a proportional damping coefficient matrix, and

$$M_{ss} = \begin{pmatrix} m & 0 & 0 \\ 0 & m & 0 \\ 0 & 0 & I \end{pmatrix} \quad (9)$$

$$K_{ss} = \begin{pmatrix} 4k & 0 & 0 \\ 0 & 4k & 0 \\ 0 & 0 & 4k \end{pmatrix} \quad (10)$$

$$K_{sb} = \begin{pmatrix} -k & 0 & -k & 0 & -k & 0 & -k & 0 \\ 0 & -k & 0 & -k & 0 & -k & 0 & -k \\ \frac{1}{2}kd & -\frac{1}{2}kd & \frac{1}{2}kd & \frac{1}{2}kd & -\frac{1}{2}kd & \frac{1}{2}kd & -\frac{1}{2}kd & -\frac{1}{2}kd \end{pmatrix} \quad (11)$$

and

$$V_g = (v_{1x} \ v_{1y} \ v_{2x} \ v_{2y} \ v_{3x} \ v_{3y} \ v_{4x} \ v_{4y})^T \quad (12)$$

where m is lumped mass, I is polar moment of inertia, k is column stiffness, d is structural dimension, and v_{ix} , v_{iy} are the ground displacement in x and y directions at support i , Fig. 1.

STOCHASTIC RESPONSE FORMULATION

Assume ground motion propagating along \bar{x} direction, Fig. 1, then ground motions in \bar{x} and \bar{y} directions can be considered statistically independent and the power spectral density functions of ground motions in \bar{y} direction are approximately 0.7 of those in \bar{x} direction (Penzien and Watabe 1975).

Ground accelerations in x and y directions can be obtained by transformation,

$$\begin{aligned} \ddot{v}_x &= \ddot{v}_{\bar{x}}\cos\alpha - \ddot{v}_{\bar{y}}\sin\alpha \\ \ddot{v}_y &= \ddot{v}_{\bar{x}}\sin\alpha + \ddot{v}_{\bar{y}}\cos\alpha \end{aligned} \quad (13)$$

where α is the angle between x and \bar{x} axes, and is defined as the ground motion incident angle.

By some tedious but otherwise straightforward derivation, the power spectral density function of the quasi-static responses in x direction can be obtained as

$$S_{x^{qs}}(\bar{\omega}) = \frac{1}{\bar{\omega}^4} |H_1(i\bar{\omega})|^2 S_0(\bar{\omega}) RT_x(\bar{\omega}, d_{kl}^l, d_{kl}^t) \quad (14)$$

where $RT_x(\bar{\omega}, d_{kl}^l, d_{kl}^t)$ is a factor function for translational responses in x direction, it has the form

$$RT_x(\bar{\omega}, d_{kl}^l, d_{kl}^t) = \frac{\cos^2\alpha + 0.7\sin^2\alpha}{8} \left[2 + \sum_{k=1}^3 \sum_{l=k+1}^4 |\gamma_{kl}(\bar{\omega}, d_{kl}^l, d_{kl}^t)| \cos(\bar{\omega}d_{kl}^l/v) \right] \quad (15)$$

The power spectral density functions for responses in y direction have the same form as Equation (14), the only difference between them is an α dependent constant factor. Therefore, only responses in x direction are discussed.

The rotational response power spectral density function is obtained as

$$S_{\theta^{qs}}(\bar{\omega}) = \frac{1}{\bar{\omega}^4} |H_1(i\bar{\omega})|^2 S_0(\bar{\omega}) RR(\bar{\omega}, d_{kl}^l, d_{kl}^t) \quad (16)$$

where

$$RR(\bar{\omega}, d_{kl}^l, d_{kl}^t) = \frac{1}{8d^2} [3.4 + 0.3(\cos^2\alpha - \sin^2\alpha)(r_{12}\cos\phi_{12} - r_{14}\cos\phi_{14} - r_{23}\cos\phi_{23} + r_{34}\cos\phi_{34}) - 1.7(r_{13}\cos\phi_{13} + r_{24}\cos\phi_{24}) + 0.6\sin\alpha\cos\alpha(r_{13}\cos\phi_{13} - r_{24}\cos\phi_{24})] \quad (17)$$

where $r_{kl}\cos\phi_{kl} = |\gamma_{kl}(\bar{\omega}, d_{kl}^l, d_{kl}^t)| \cos(\bar{\omega}d_{kl}^l/v)$.

The power spectral density functions of the dynamic and total structural responses in x direction can be derived as

$$S_{x^d}(\bar{\omega}) = \bar{\omega}^4 |H_x(i\bar{\omega})|^2 S_{x^{qs}}(\bar{\omega}) \quad (18)$$

and

$$S_{x^t}(\bar{\omega}) = \omega_0^4 |H_x(i\bar{\omega})|^2 S_{x^{qs}}(\bar{\omega}) \quad (19)$$

where $|H_x(i\bar{\omega})|^2$ is a transfer function for translational response mode

$$|H_x(i\bar{\omega})|^2 = \frac{1}{(\omega_0^2 - \bar{\omega}^2)^2 + 4\xi^2\omega_0^2\bar{\omega}^2} \quad (20)$$

where $\omega_0 = \sqrt{\frac{4k}{m}}$ is natural frequency, ξ is damping ratio.

The dynamic and total rotational response power spectral density functions can be derived as

$$S_{\theta^d}(\bar{\omega}) = \bar{\omega}^4 |H_\theta(i\bar{\omega})|^2 S_{\theta^{qs}}(\bar{\omega}) \quad (21)$$

and

$$S_{\theta^t}(\bar{\omega}) = \omega_\theta^4 |H_\theta(i\bar{\omega})|^2 S_{\theta^{qs}}(\bar{\omega}) \quad (22)$$

where $\omega_\theta = \sqrt{\frac{2kd^2}{I}}$ is natural frequency for rotational mode, $|H_\theta(i\bar{\omega})|^2$ is corresponding transfer function.

The power spectral density functions of the acceleration responses can be obtained by multiplying the corresponding displacement response spectra by $\bar{\omega}^4$. The variances of the responses can be obtained by integrating the power spectral density functions.

NUMERICAL RESULTS

Structural response variances are calculated. The parameters used are $\xi_g = 0.6$, $\omega_g = 5\pi$ rad/s, $d = 100m$, $v = 1000m/s$, $S = 10^7$ cm²/s² and $\alpha = 30^\circ$. The translational responses are normalized by the corresponding responses from single input. Rotational responses to single ground motion input are zero. The results for the three cases are presented and compared.

Fig. 2 shows quasi-static responses with respect to d/v . It can be seen that the ratios of all the responses decreases as d/v increases. The multiple input effect to translational responses are dominated by ground motion phase shift effects, while coherency loss effects are more critical to rotational displacement responses.

Fig. 3 shows dynamic responses with respect to a dimensionless parameter f_0/f_d , where f_0 is natural frequency of the system and $f_d = v/d$ is wave frequency of wavelength d . It can be seen that single input assumptions overestimate translational responses and underestimate rotational responses. By comparing with the general input results (Case 1), it can be concluded that the translational responses are always overestimated while the rotational responses are always underestimated by neglecting phase shifts effects, and the responses are sometimes underestimated and sometimes overestimated by neglecting coherency loss effects.

Fig. 4 shows total responses with respect to f_0/f_d . It can be seen that the total displacements are overestimated by either neglecting the phase shift or coherency loss effects, while accelerations are underestimated by neglecting phase shift effects, but sometimes overestimated and sometimes underestimated by neglecting coherency loss effects.

From Equations (14) to (22), it can be noticed that the critical incident angle α to translational responses is either 0° or 90° . But the critical α to rotational responses depends on the coherency properties. Fig. 5 shows the comparisons between the total responses from the ground motions with different incident angles α . It can be seen that all the responses, except rotational accelerations, are reduced if $\alpha \neq 0$. For rotational accelerations, the total responses vary with the incident angles.

CONCLUSIONS

Single input representations of the ground motions always overestimate translational responses but underestimate rotational responses. By considering the ground motion phase shifts only, structural responses are sometimes overestimated and sometimes underestimated. By considering ground motion coherency loss effects only, translational responses are overestimated and rotational responses are underestimated. The ground motion incident angles also affect structural responses. The total responses are generally reduced by a non zero incident angle except for the responses of rotational accelerations.

REFERENCES

- Harichandran, R.S. and Vanmarcke, E. 1984, Space-Time Variation of Earthquake Ground Motion. Research Report R84-12, Dept. of Civil Engrg., Massachusetts Institute of Technology.
- Hao, H., Oliveira, C.S. and Penzien, J. 1989, Multiple-Station Ground Motion Processing and Simulation Based on SMART-1 Array Data. Nuclear Engineering and Design, Vol. 111, 293-310.
- Harichandran, R.S. and Wang, W. 1988, Response of Simple Beam to Spatially Varying Earthquake Excitation. J. of Engrg. Mech., ASCE, Vol. 114, No. 9, 1526-1541.
- Harichandran, R.S. and Wang, W. 1990, Response of Indeterminate Two-Span Beam to Spatially Varying Seismic Excitation. Earthq. Engrg. and Str. Dyn., Vol. 19, 173-187.
- Zerva, A. 1990, Response of Multi-Span Beams to Spatially Incoherent Seismic Ground Motions. Earthq. Engrg. and Str. Dyn., Vol. 19, 819-832.
- Hao, H. 1991, Response of Multiply-Supported Rigid Plate to Spatially Correlated Seismic Excitations. Submitted for Review for Publication in Earthq. Engrg. and Str. Dyn..
- Hao, H. 1989, Effects of Spatial Variation of Ground Motions on Large Multiply-Supported Structures. Report No. EERC 89-06, Earthquake Engineering Research Center, University of California, Berkeley.

Ruiz, P. and Penzien, J. 1969, Probabilistic Study of the Behavior of Structures during Earthquakes. Report No. EERC 69-03, Earthquake Engineering Research Center, University of California, Berkeley.
 Tajimi, H. 1960, A Statistical Method of Determining the Maximum Response of a Building Structure During an Earthquake. Proc. 2WCEE, Vol. 2, Tokyo, 781-797.
 Penzien, J. and Watabe, M. 1975, Characteristics of 3-Dimensional Earthquake Ground Motions. Earthq. Engrg. and Str. Dyn., Vol. 3, 365-373.

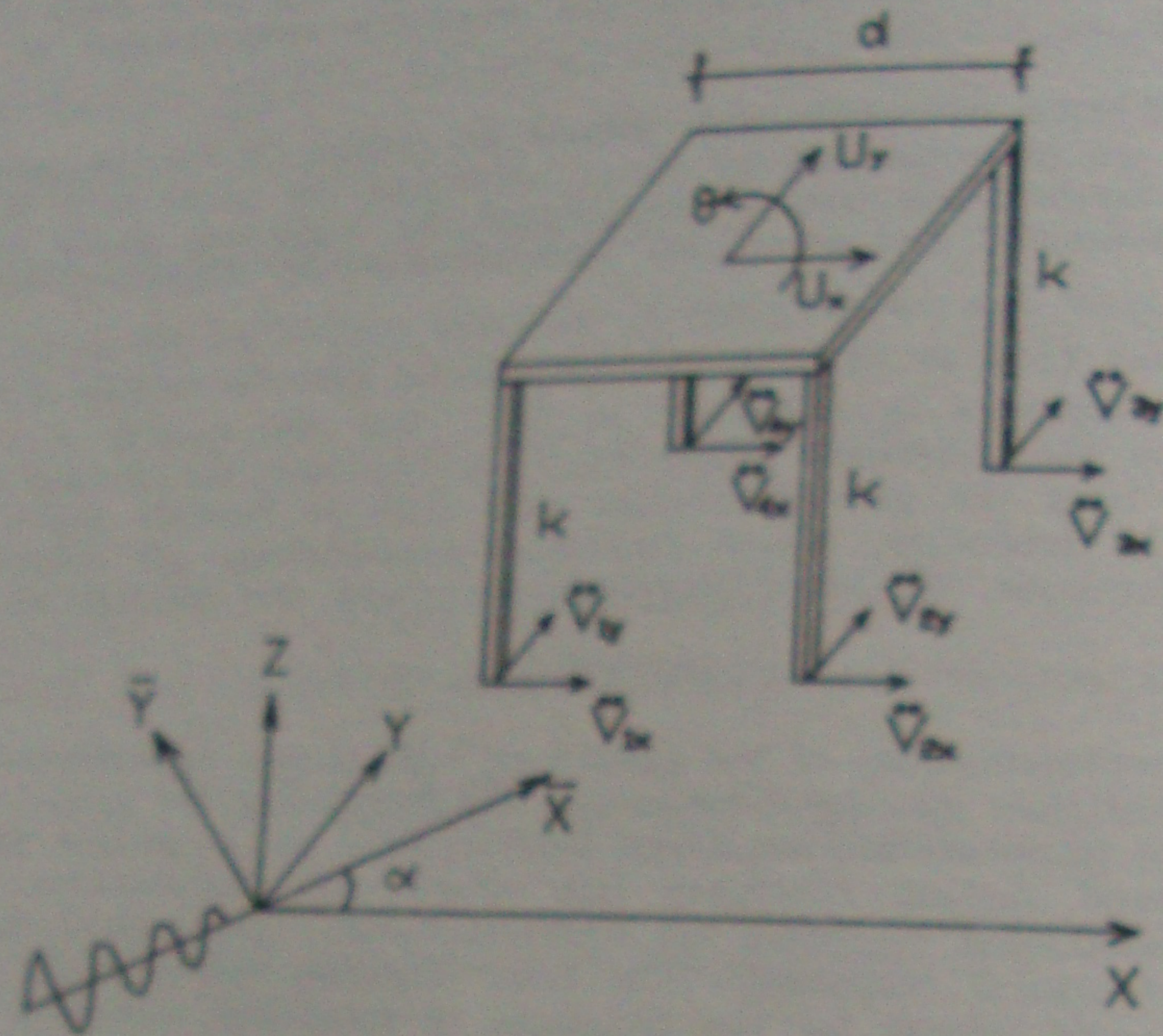


Figure 1. Multiply-supported rigid plate

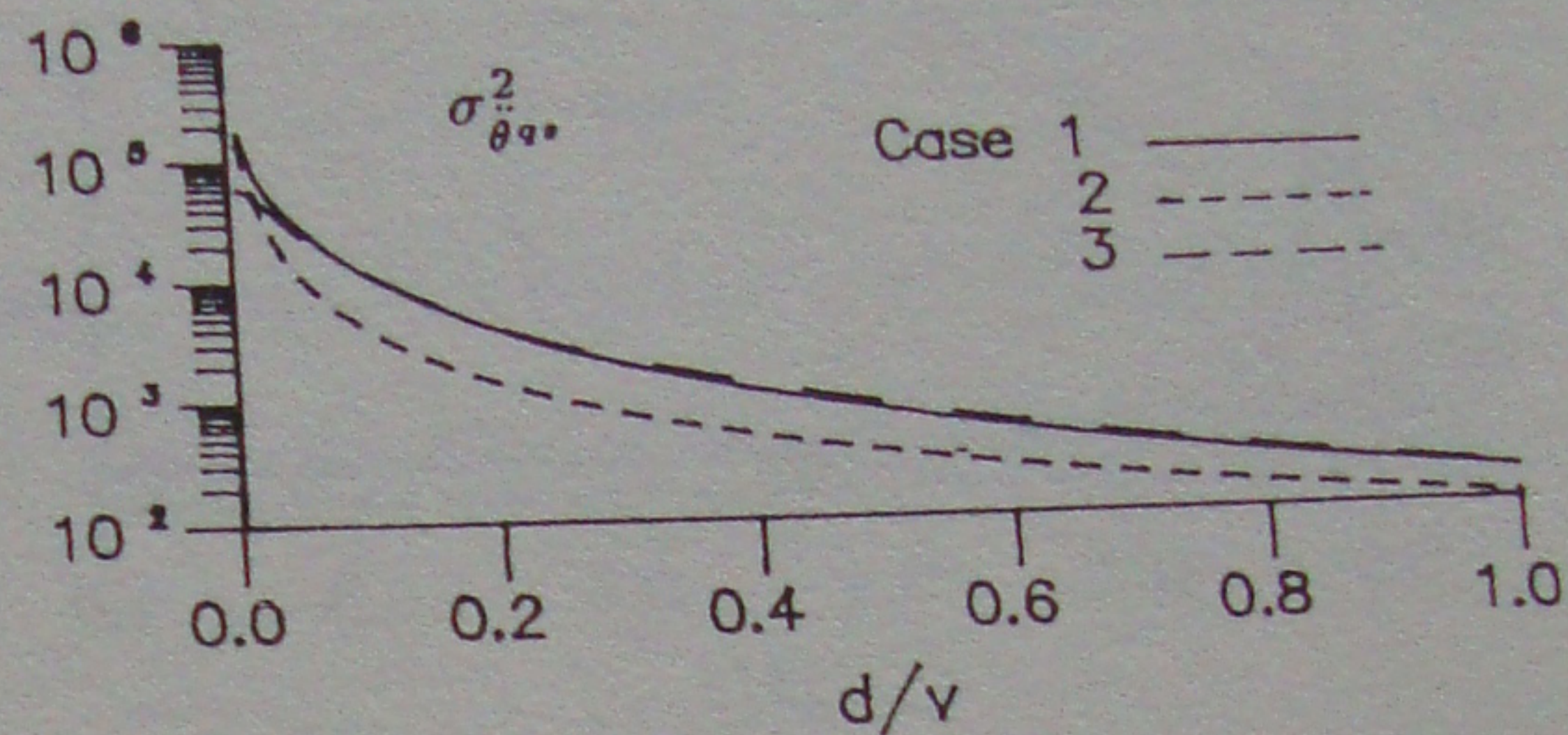
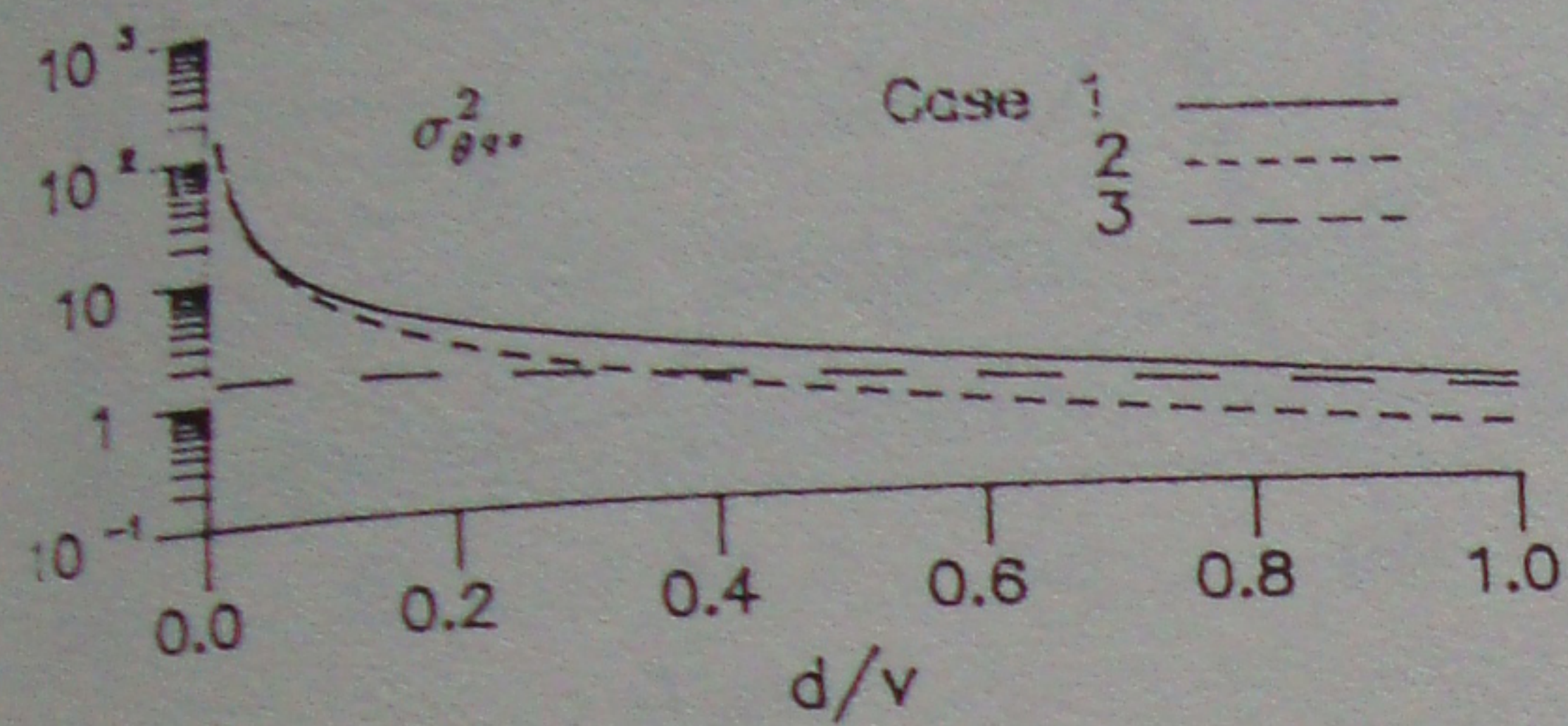
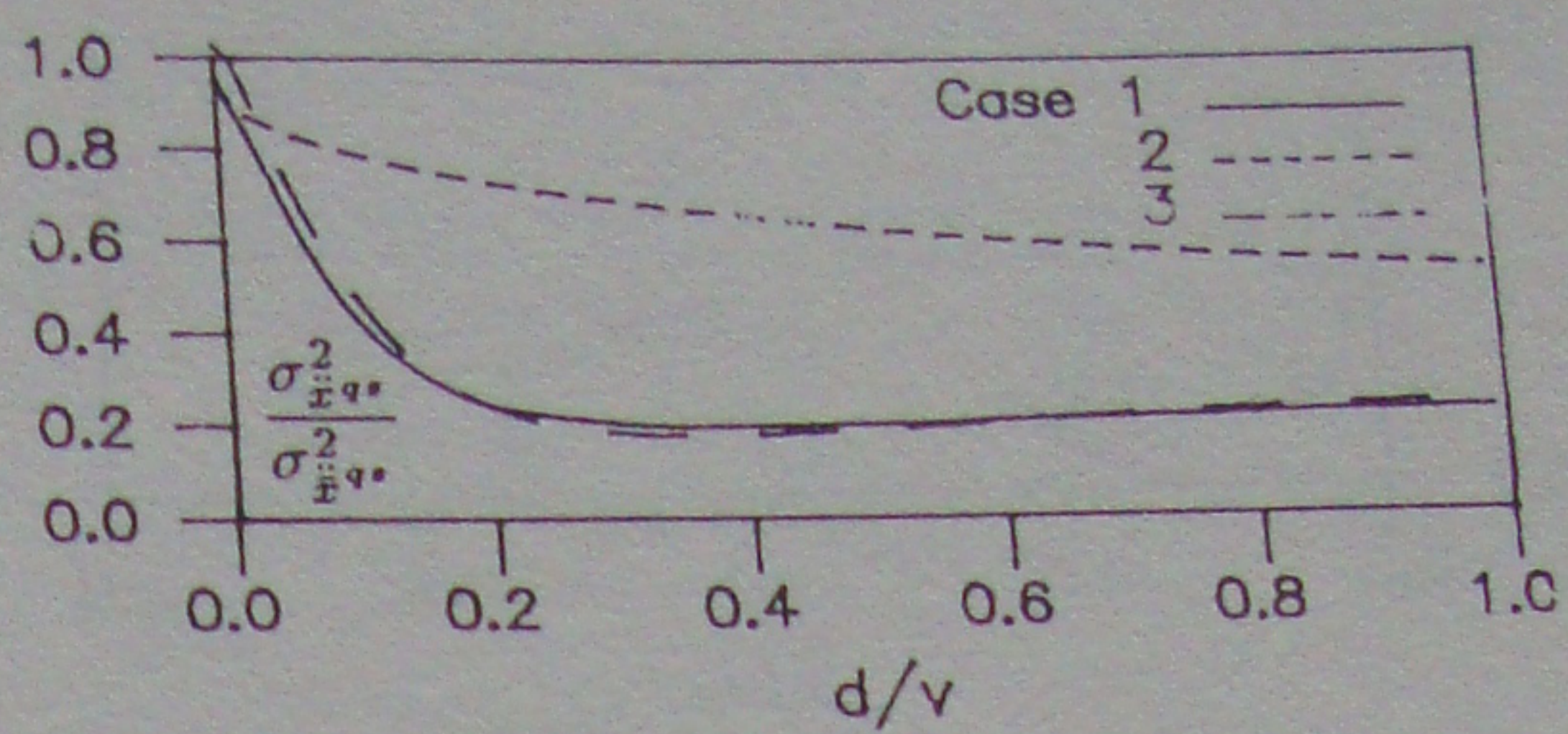
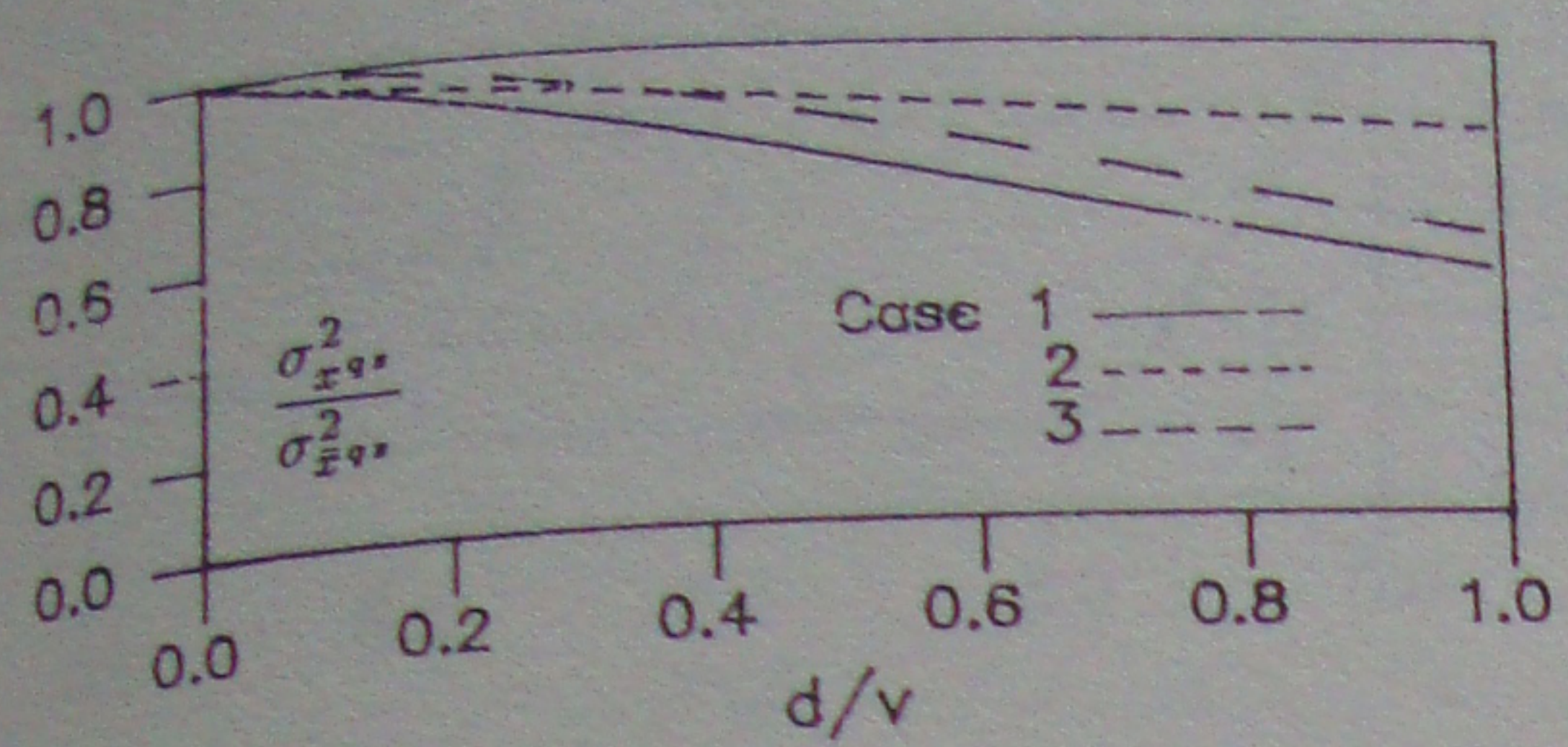


Figure 2. Quasi-static response variances

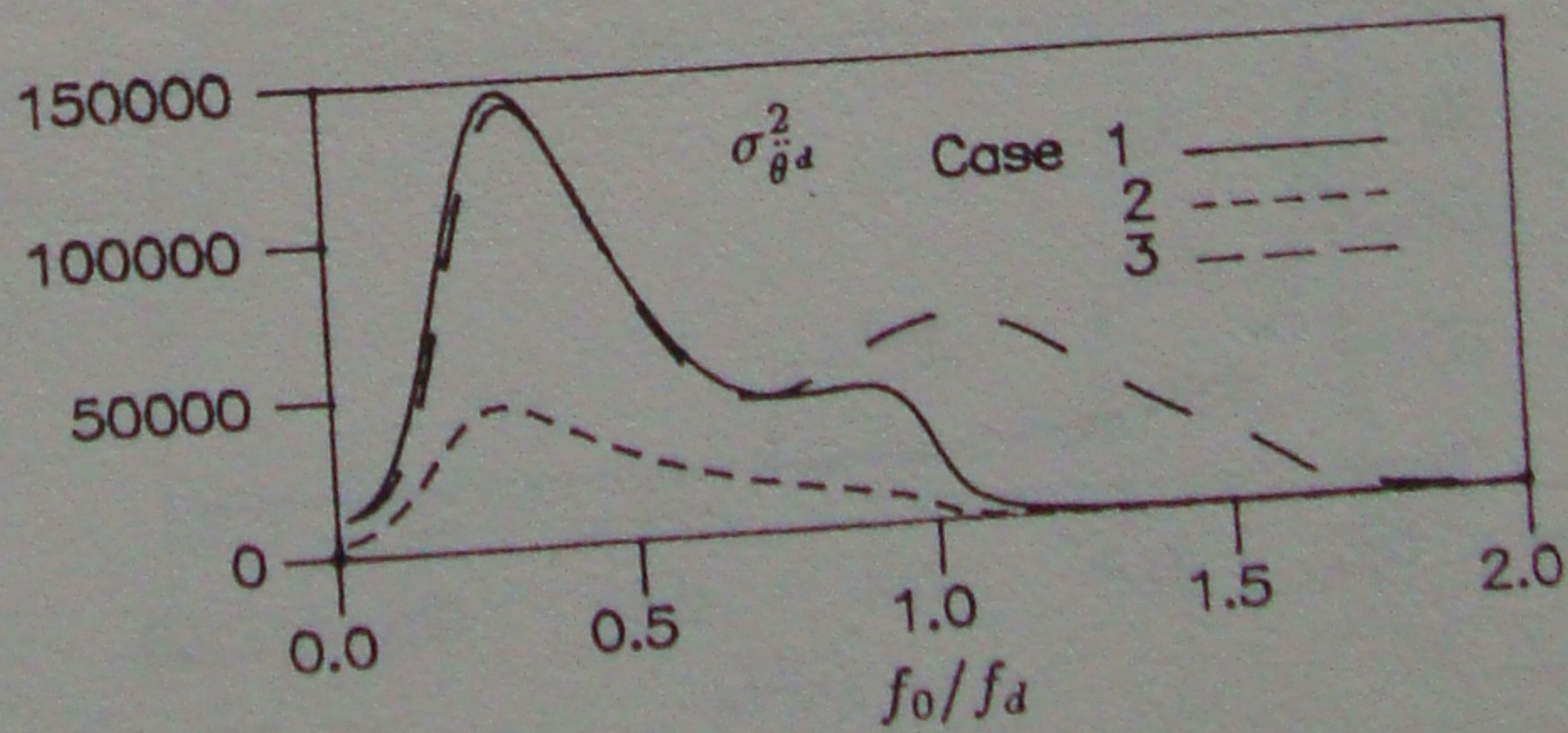
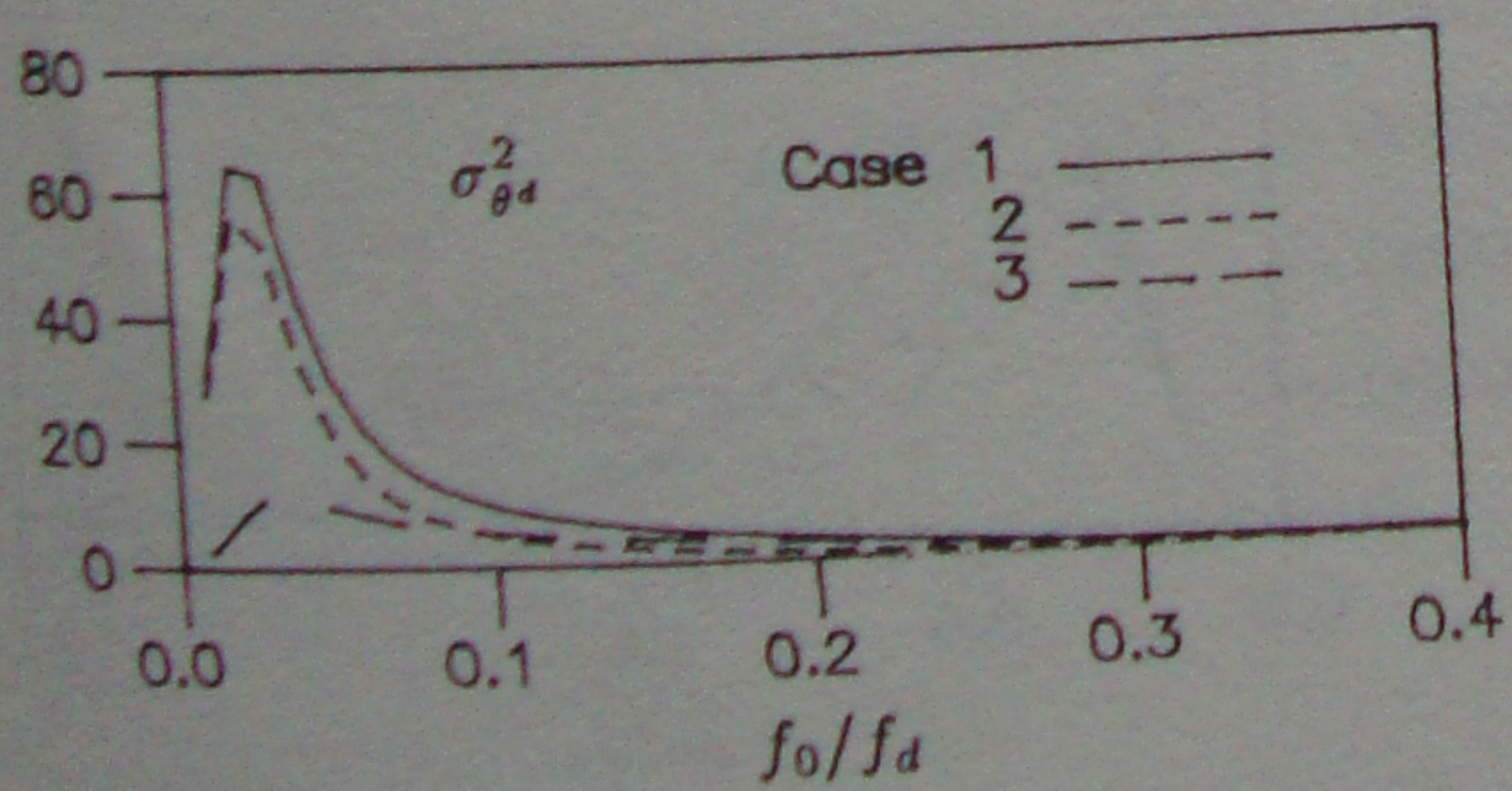
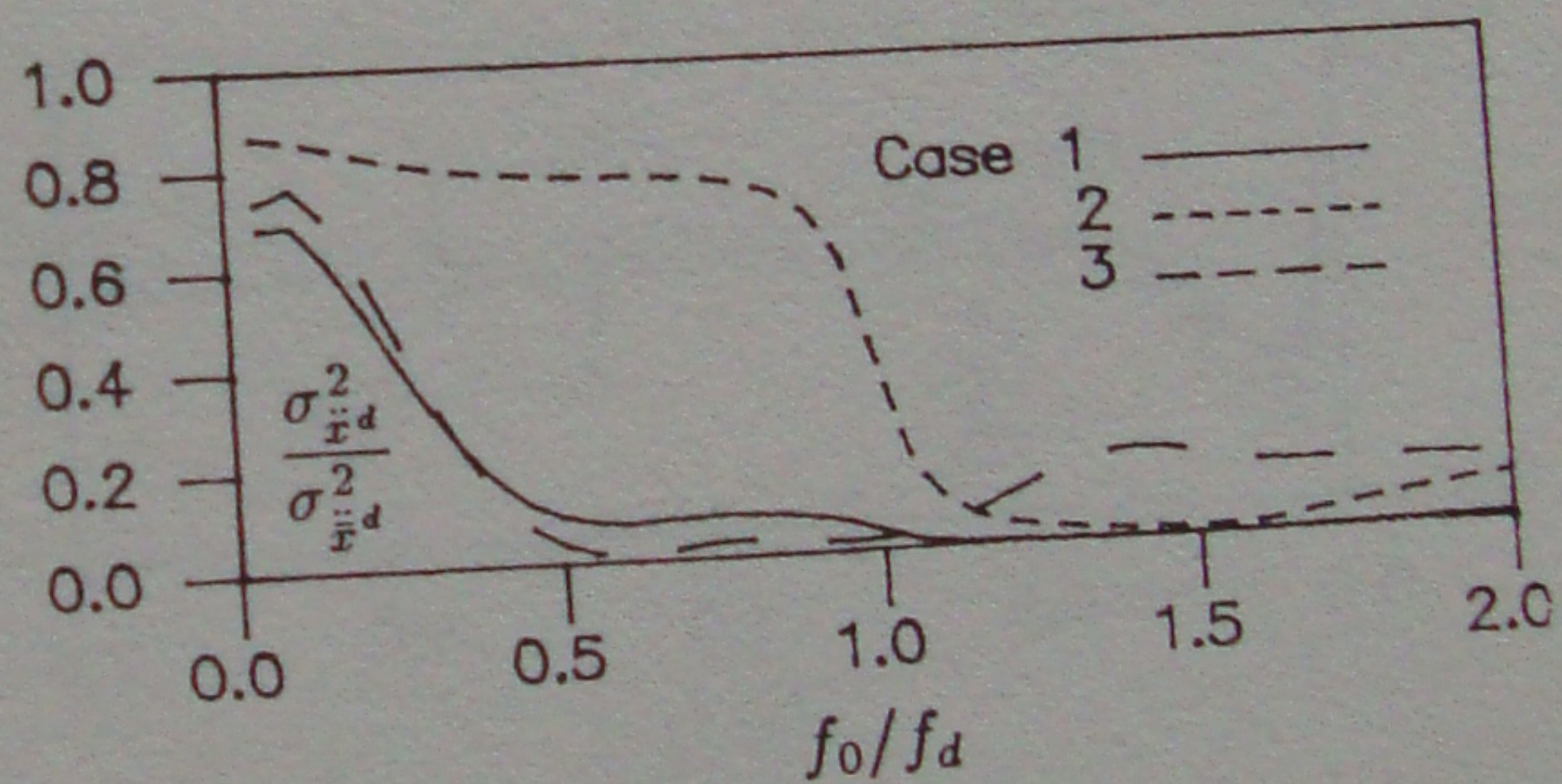
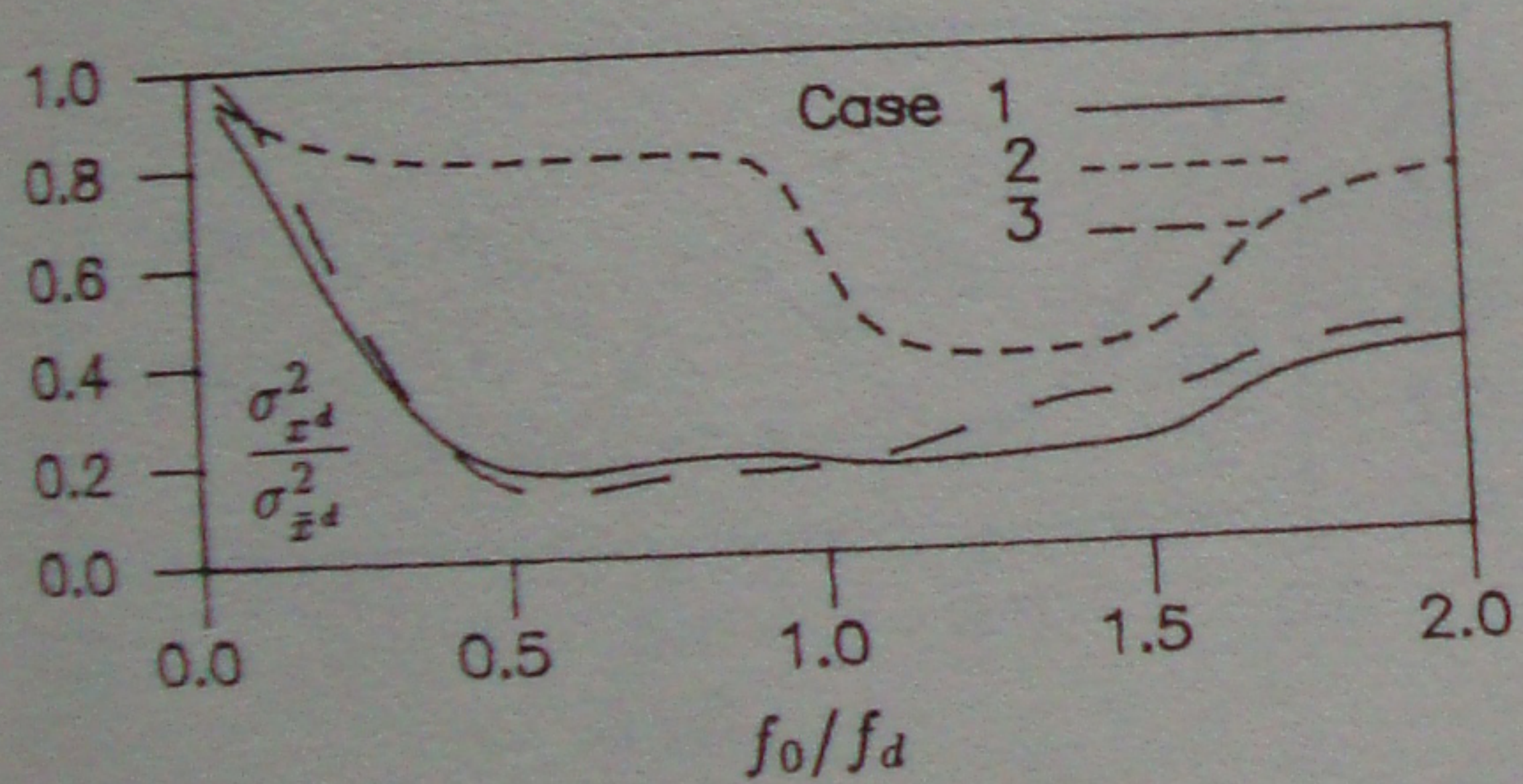


Figure 3. Dynamic response variances

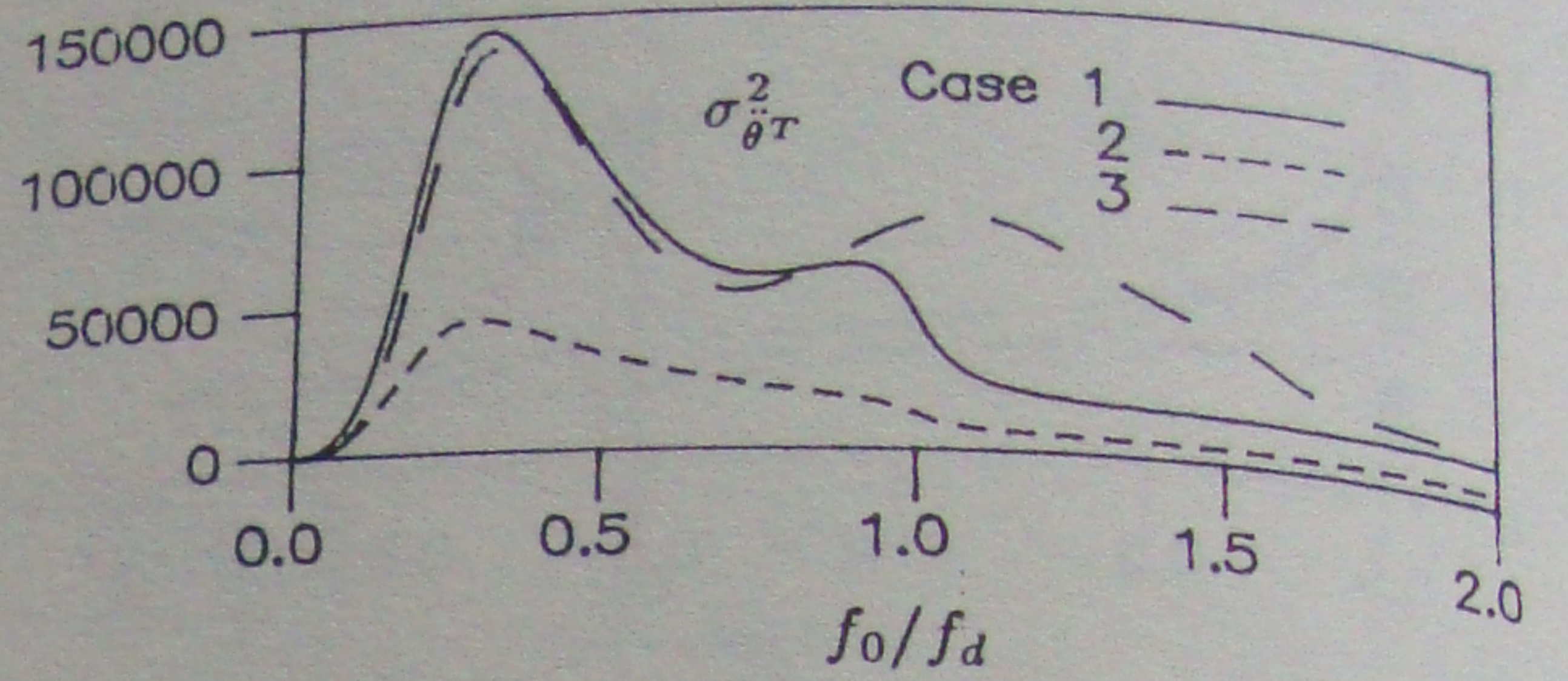
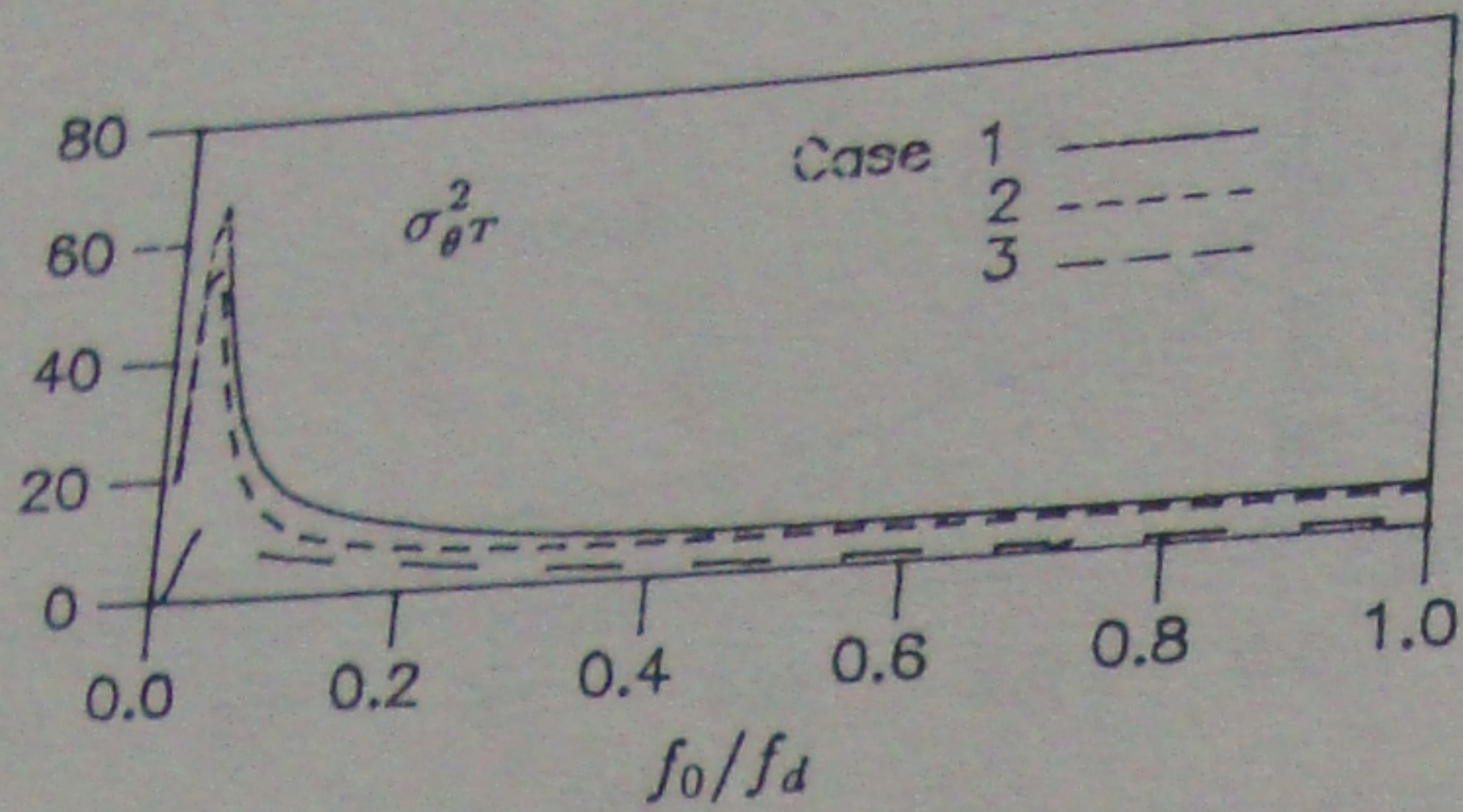
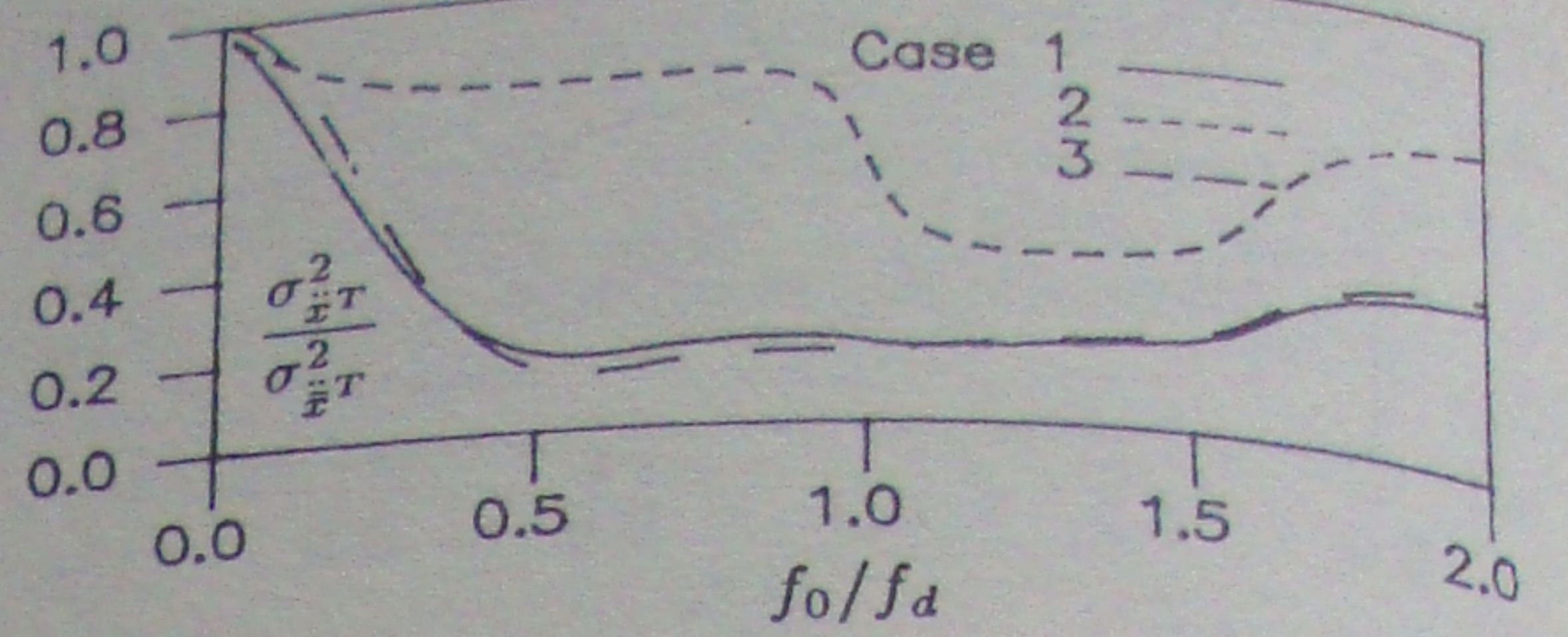
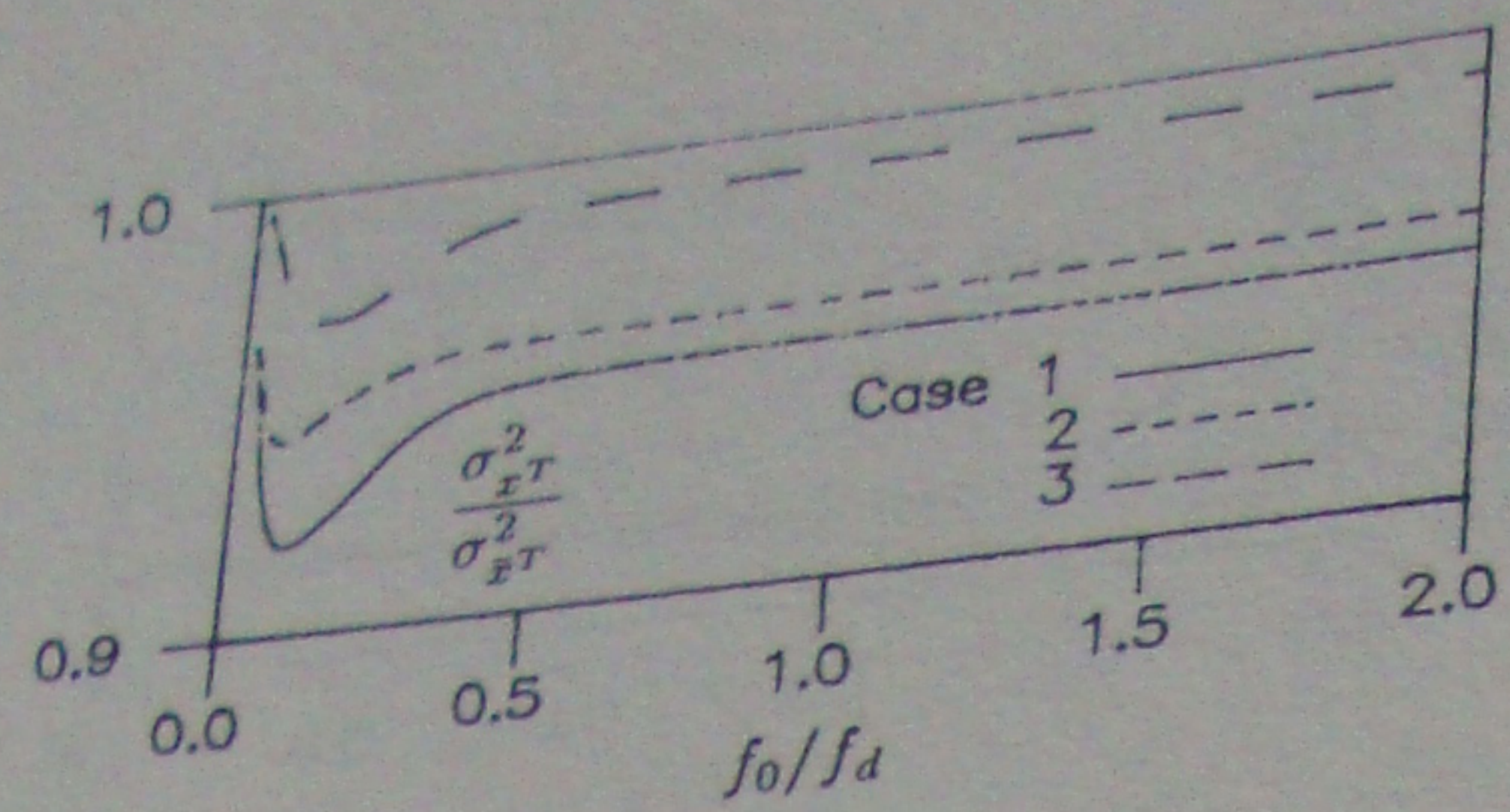


Figure 4. Total structural response variances

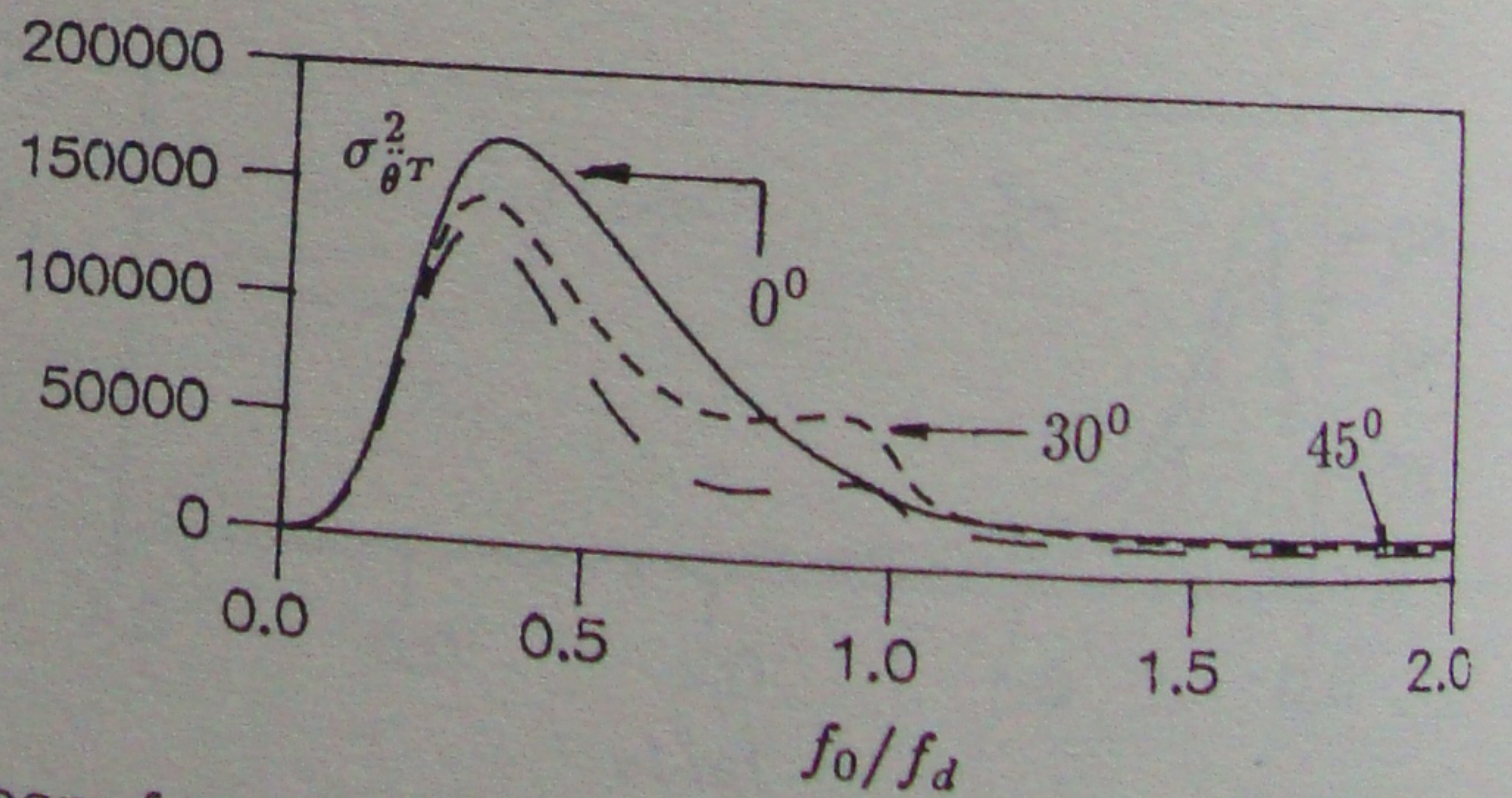
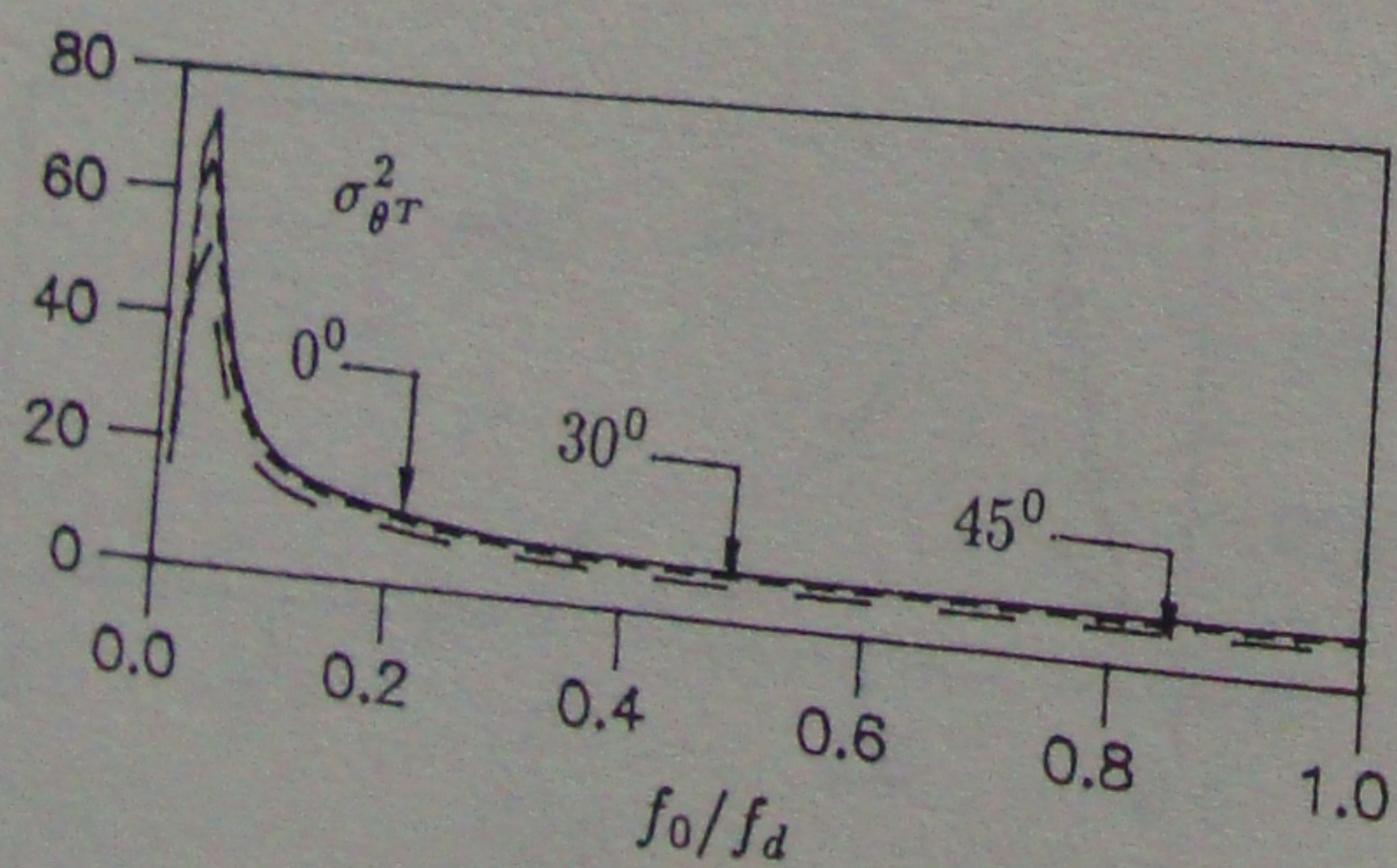
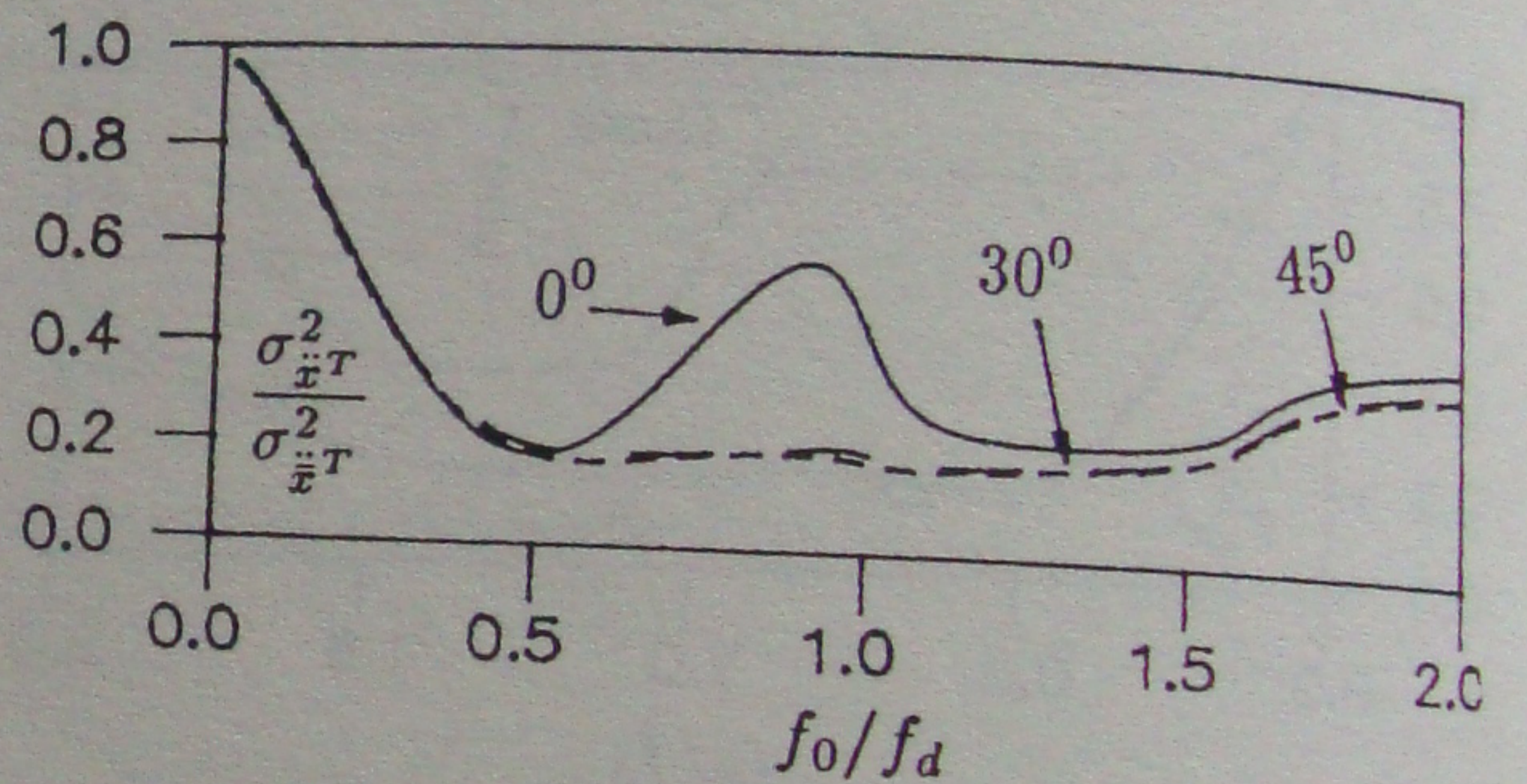
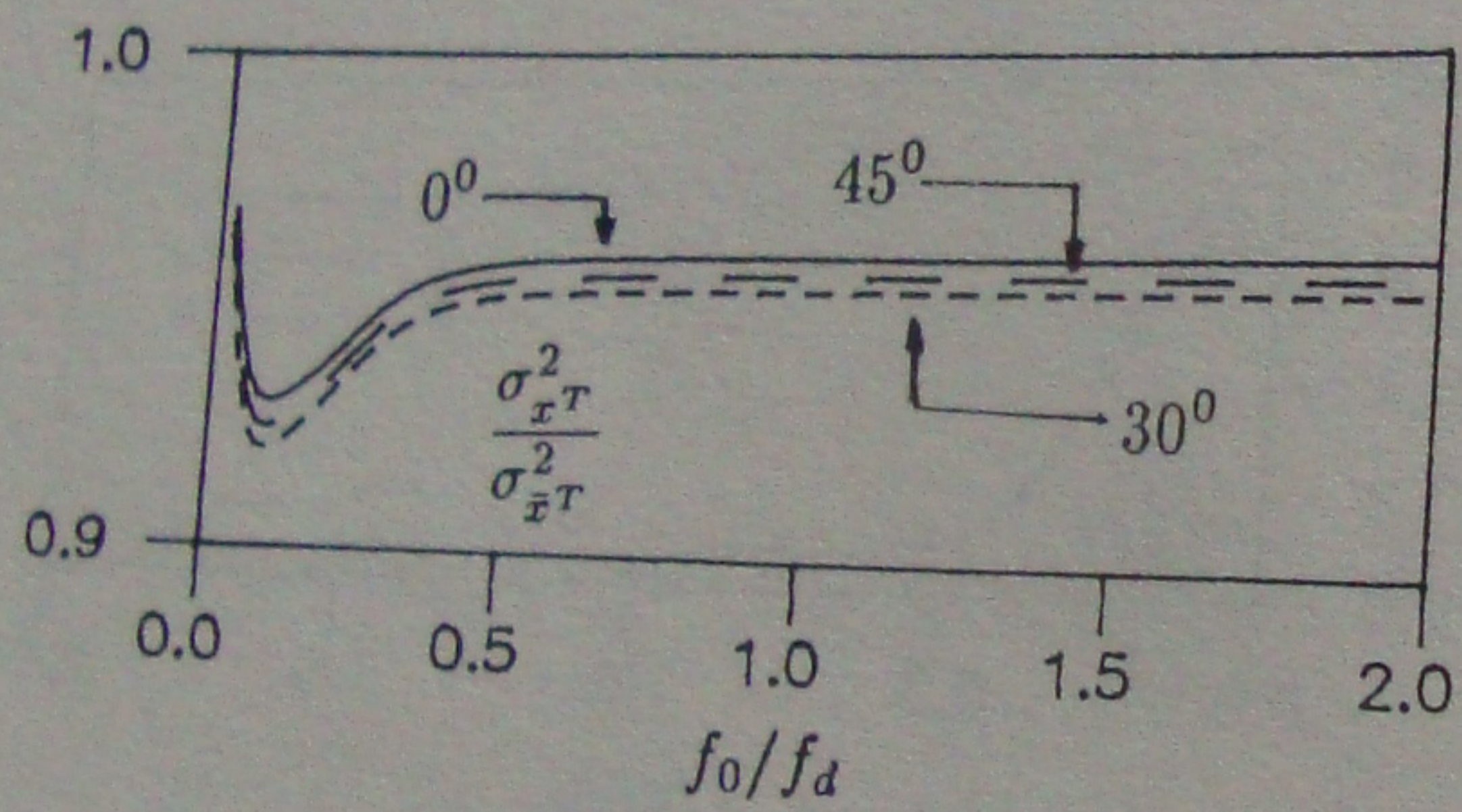


Figure 5. Total response variances for different incident angles